

Fast Design Space Exploration of Nonlinear Systems: Part I

Sanjai Narain, Emily Mak, Dana Chee, Brendan Englot, Kishore Pochiraju, Niraj K. Jha, Karthik Narayan

Abstract— System design tools are often only available as blackboxes with complex nonlinear relationships between inputs and outputs. Blackboxes are intended to be run in the forward direction: for a given design as input they compute an output representing system behavior. Most cannot be run in reverse to produce an input from requirements on output. Thus, finding a design satisfying a requirement is often a trial-and-error process without assurance of optimality. Finding designs concurrently satisfying a set of requirements is harder because designs satisfying individual requirements may conflict with each other. Compounding the hardness are the facts that blackbox evaluations can be expensive and sometimes fail to produce an output due to non-convergence of underlying numerical algorithms. This paper presents CNMA¹, a new constrained optimization method for blackboxes. It is conservative in the number of blackbox evaluations. Any designs it finds are guaranteed to satisfy all requirements. It is resilient to the failure of blackboxes to compute outputs. CNMA tries to sample only the part of the design space relevant to solving the design problem, leveraging the power of neural networks, Mixed Integer Linear Programs, and a new learning-from-failure feedback loop. The paper also presents a parallel version of CNMA that improves the efficiency and quality of solutions over the sequential version, and tries to steer it away from local optima. CNMA’s performance is evaluated for seven nonlinear design problems of 8 (two problems), 10, 15, 36 and 60 real-valued dimensions and one with 186 binary dimensions. It is shown that CNMA improves the performance of stable, off-the-shelf implementations of Bayesian Optimization and of Nelder Mead and Random Search by 1%-87% for a given fixed time and function evaluation budget. Note, however, that these implementations did not always return solutions.

Index Terms— Blackbox optimization; constrained optimization; Mixed-Integer Linear Program (MILP); neural networks; optimization; sample efficiency.

I. INTRODUCTION

System design knowledge is often encapsulated inside blackboxes such as simulators, spreadsheets and program scripts. Blackboxes are, typically, nonlinear functions that accept a design as input and produce a representation of system behavior as output. A central design problem is producing an input from requirements or constraints on blackbox output.

Relevant to solving this “inverse problem” are the mature, constrained nonlinear optimization methods [1, 2, 3, 4, 5, 6, 7, 8, 9, 10]. Also available is a large online collection of these methods [11] along with a companion guide [12]. These methods optimize an objective function subject to constraints. These fall into two categories: derivative-based and derivative-free. The former compute derivatives of the objective-function

to determine the direction in which to search for a point where the derivative becomes zero. They are restricted to smooth, continuous functions. Moreover, derivative computation is not sample-efficient and thus infeasible when objective function evaluation is expensive as is often the case for blackboxes.

Derivative-free methods [5, 7] are conservative in the number of times they evaluate functions. One class of such methods is called *direct search* whose well-known members include Nelder-Mead (NM) [6] and COBYLA [13]. They maintain a simplex (convex hull) of points around the current point and use this to compute the next point to sample in the direction of the optima. These methods require starting points whose incorrect choices can cause the methods to be stuck in local optima.

Surrogate-based methods are another class of derivative-free methods [7, 8]. Examples include Bayesian Optimization (BO) with Gaussian Processes (BO/GP) [9] and Alamo [3]. They do not require starting points. Instead, they start from a set of samples, construct a surrogate (model) of the objective function over its whole domain, and from it construct a merit or acquisition function. This merit function is optimized to compute the best point to sample next. If this point does not satisfy a halting condition, the point is added to the set of samples and the search is restarted. In earlier BO/GP versions, the complexity of building surrogate functions was cubic in the number of samples [1] although faster versions on GPUs are reported in [14]. To optimize with constraints, various extensions to BO/GP have been presented in [15, 16, 17, 18]. Parallel BO/GP algorithms have been presented in [19, 20, 21].

The above methods can be susceptible to failure of objective functions to evaluate, as can happen, for example due to non-convergence of computational fluid dynamics simulators [22]. If an artificial value has to be assigned to the function it could distort the simplexes and surrogates.

Many of the above methods handle constraints indirectly by reducing constrained optimization with a sequence of one or more unconstrained optimization problems [2, 4, 23, 24]. The principle is to encode the cost of violating a constraint as a penalty/barrier function and rely on an optimization engine to drive this cost to zero. For example, to model the constraint $x \leq 1$, the term $\max(0, x - 1)$ can be added to the objective function. Whenever $x > 1$, the term would evaluate to a positive number. Hence, the optimization engine (doing minimization) would search in a region where the cost is zero. However, such functions can distort the shape of the new objective function making it harder to find the optima. Reducing such distortion requires substantial creativity on the part of the penalty/barrier function designer [4, 25].

This work was done under a contract from the Defense Advanced Research Projects Agency (DARPA) and Air Force Research Laboratory (AFRL). The views, opinions and/or findings expressed are those of the authors and should not be interpreted as representing the official views or policies of the Department of Defense or the U.S. Government. Distribution A. Approved for Public Release, Distribution Unlimited.

Sanjai Narain, Emily Mak and Dana Chee are with Perspecta Labs (e-mail:

snarain@perspectalabs.com), Basking Ridge, NJ, Brendan Englot and Kishore Pochiraju are with Stevens Institute of Technology, Niraj K. Jha is with Princeton University and Karthik Narayan with Starfruit-LLC.

¹ Constrained optimization with Neural networks, MILP solvers and Active learning.

This paper presents CNMA, a new surrogate-based method for solving the inverse problem for blackboxes. Formally, CNMA finds values of x, y that optimize $\phi(x, y)$ such that $F(x) = y \wedge P(x, y)$ where F is a potentially nonlinear function available as a blackbox, x, y are vectors of discrete and continuous variables, ϕ is a linear function and P is a linear constraint. P can also be a conjunction of several constraints. Note that \wedge denotes logical conjunction (AND). As shown in Section V.H, nonlinear objective functions and constraints can be handled by moving their nonlinearities inside the definition of F .

CNMA’s innovation is connecting the modeling power of neural networks and constraint-solving power of MILP solvers into a learning-from-failure feedback loop in such a way that they do much of the work for us, permitting straightforward, efficient implementations of the following desirable features into a single, cohesive system:

1. **Efficient construction of a surrogate function.** The complexity of neural network is linear with the number of samples.
2. **Efficient constraint-solving without penalty functions.** This feature is enabled by the transformation of neural networks with the ReLU activation function into an equivalent MILP. In addition, constraints are directly expressed in the MILP language and then efficiently solved by industrial-strength MILP solvers such as CPLEX and Gurobi [11, 12].
3. **Sample efficiency.** This feature is enabled by CNMA’s learning-from-failure feedback loop. A surrogate is learnt as a neural network that is then transformed into a MILP. Using this MILP, a constrained optimization problem is solved and if the solution is unacceptable, it is used to find a new point to sample.
4. **Optimization with discrete and continuous variables.** Function inputs, outputs and constraints can all contain discrete and continuous variables. This feature is enabled by the use of both neural networks and MILP solvers.
5. **Solving constraints whose evaluation itself requires blackbox evaluations.** CNMA handles this by introducing new variables for components of constraints that must be evaluated via blackbox methods and shifts the blackbox estimation to the underlying surrogate that is created. See Section V.H.
6. **Resilience to the failure of blackboxes to compute outputs.** CNMA leverages the ability of neural networks to learn despite missing information. It makes no assumptions about function continuity or smoothness. In Figure 1 is shown an example of a function CNMA can optimize over.
7. **Parallelism.** A simple parallel version of CNMA, also presented in this paper, improves the efficiency and quality of solutions over the sequential version, and also tries to steer it away from local optima. No restriction is placed on functions that can be optimized in parallel.

CNMA samples points in the domains of the function, and learns a neural network surrogate of the function. By the Universal Approximation Theorem [26], neural networks can approximate any continuous function, although in practice, they are also used to approximate non-continuous, non-smooth

functions. CNMA transforms that surrogate into an equivalent MILP [27] and constructs its conjunction with $P(x, y)$. It optimizes $\phi(x, y)$ subject to this conjunction using industrial-strength MILP solvers. It then checks the solution for correctness, i.e., whether it satisfies $P(x, y)$ and whether the objective function is of acceptable value. If so, CNMA outputs the solution. If not, CNMA computes a new training instance from the solution and restarts. This “learning-from-failure” feedback loop has the effect of trying to sample the region of the domain relevant to solving the optimization problem. Thus, it reduces the number of function evaluations by orders of magnitude compared to that needed for learning the function over its entire domain.

By contrast, methods in [28, 29] learn the function over its entire domain as a neural network and use it as a fast evaluator

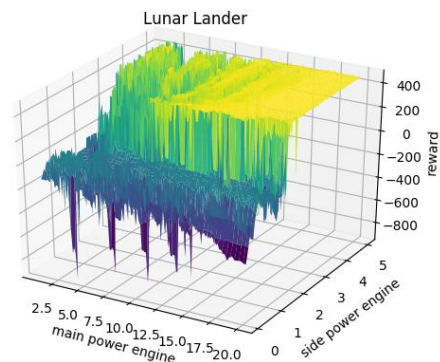


Figure 1. An example of a function over which CNMA can optimize. It is non-continuous and not even defined at all points. Only two dimensions of the 15 are shown. See Section V.B for details.

for other optimization algorithms. These methods may not be practical when blackbox evaluation is expensive and even when not, the number of samples needed to model a function accurately enough can be astronomical.

A parallel version of CNMA uses multiple agents with each using a different neural network architecture but operating off the same training set. Each independently computes the next best point to sample and adds it to the common training set. The resulting model diversity decreases the chances of getting stuck in local optima. Parallel neural network training, MILP solving and sample evaluation also contribute to improved performance over the sequential version.

Genetic algorithms [30] can be combined with CNMA in a form of hybrid optimization to find solutions that may not be found by one or the other alone. This idea is thoroughly explored in a sister paper of the same title but Part II [31].

The paper is organized as follows. Section II discusses related work, in particular, highlighting the relationship of CNMA with BO/GP. Section III provides the necessary background. Section IV presents sequential and parallel CNMA and illustrates them with a simple example. Section V evaluates CNMA performance for seven nonlinear problems of 8 (two problems), 10, 15, 36 and 60 real-valued dimensions and one with 186 binary dimensions. Its performance is compared with that of the `skopt` [32] implementation of BO/GP (abbreviated BO-S) and the `scipy.optimize` [33] implementation of NM (abbreviated NM-S), and Random

Search. BO-S and NM-S are stable, off-the-shelf tools. Note, however, that BO-S did not return a solution for two problems and NM-S did not return one for three. Section VI concludes the paper.

II. RELATED WORK

Surrogate-based methods are most closely related to CNMA. Of these methods, perhaps the most well-researched is BO/GP [9]. Let the objective function to be maximized be $F(x)$ and let a blackbox be available to evaluate $F(x)$. BO/GP is initialized with a covariance function $k(x, y)$, also called a kernel. BO/GP is also initialized with a set S of samples in the domain of F and their associated values. With this information, BO/GP iteratively updates the posterior distribution of the underlying Gaussian Process, parameterized by $\mu(x)$ and $\sigma(x)$. Intuitively, $\mu(x)$ is the mean of the values at x , of all possible functions whose value for any sample v in S is $F(v)$. $\sigma(x)$ is the standard deviation of all these values. These two functions are combined in different ways to create a merit or acquisition function. This function is maximized using an optimization engine such as L-BFGS [34]. The value of x in the solution represents a new point to sample, relevant to the optimization problem that balances exploration with exploitation. It is added to S and the step repeats till a sample satisfying some halting condition is found. One such acquisition function is the Upper Confidence Bound $UCB(x) = \mu(x) + \beta * \sigma(x)$ with $\beta \geq 0$. The construction of $\mu(x)$ and $\sigma(x)$ requires the inversion of the covariance matrix that lists $k(u, v)$ for each pair (u, v) where u, v are samples in S . In earlier versions of BO/GP, a matrix inversion method cubic in the number of samples was used [1], although faster methods on GPUs are reported in [14].

If $F(x)$ is to be optimized subject to a constraint $P(x, F(x))$, $P(x, F(x))$ could be modeled as a penalty/barrier function and added to $F(x)$. If $P(x, F(x))$ itself requires a blackbox evaluation, extensions of BO/GP have been proposed [15, 16, 17, 18] that, in their inner loop, find an x for which the likelihood of $F(x)$ being the maximum and that of $P(x, F(x))$ being true is high.

Parallel versions of BO/GP have been proposed in [19, 20, 21]. Some, such as ref. [19], assume function “additivity,” i.e., the function can be decomposed into a sum of functions on disjoint subsets of the function domain. In ref. [35] is reported the use of a neural networks as a surrogate but the surrogate remains inside the Gaussian Processes framework. It is not solved with a MILP solver. In ref. [36] is reported a scheme for mixed discrete-continuous variables in BO/GP. To handle failure of function evaluation, ref. [37] reports a scheme for learning problematic areas of the search space and avoiding it.

Like BO/GP, CNMA also builds a surrogate of $F(x)$, say $F_{nn}(x)$, from sampling the blackbox. The selection of the neural network architecture is analogous to selection of the kernel and $F_{nn}(x)$ is analogous to $\mu(x)$. The MILP solver is analogous to an engine such as L-BFGS. It is directly used to find x that maximizes y such that $F_{nn}(x) = y \wedge P(x, y)$. Any solution is used to compute the next point to sample.

Connecting neural networks and MILP solvers in a learning-from-failure feedback loop permits efficient, straightforward implementation of above features: efficient surrogate function construction, sample efficiency, constraint solving without

penalty functions, solving blackbox constraints, optimization with discrete and continuous variables, resilience to non-terminating function evaluations, and parallelism.

CNMA does not compute the variance of the surrogate it learns. Effectively, its merit function is $UCB(x)$ with $\beta = 0$. There is, thus, a risk that it could get stuck in local optima finding more and more points around the current optima. CNMA provides two methods for trying to avoid this problem and searching globally. The first is to use a constraint stating that the objective function is above a threshold. Then, the MILP solver will not produce solutions for which the objective is below the threshold. The second is to introduce model diversity to reduce the chances of different models computing the same local optima. Model diversity is a byproduct of parallel CNMA whose multiple agents create their own models. Independently, parallel CNMA also contributes to improved performance via parallel neural network training, MILP solving and sample evaluation.

If the current surrogate is not good enough then $F_{nn}(x)$ subject to $P(x)$ may have no solution. In that case, CNMA generates a random point and restarts. How to mitigate such randomness is one problem of current research. Other future research problems include introducing additional diversity, e.g., by use of bootstrapping, multi-function CNMA, finding an appropriate initial neural network architecture and adapting that architecture as new samples are created, e.g., via the use of network compression [38].

We now discuss CNMA in detail.

III. BACKGROUND

A mixed-integer linear constraint is of the form $a_0 * x_0 + \dots + a_k * x_k \leq b$ where a_i, b are real-valued constants and the x_i are real-valued or integer-valued. An MILP is a set of such constraints with a linear objective function $\phi(v_0, \dots, v_m)$ where each v_i is a variable appearing in a constraint. An MILP solver finds values of all variables in the program optimizing the function while satisfying all constraints. It makes no distinction between input and output variables.

A neural network is a set of layers with each layer consisting of a set of neurons. In the fully-connected neural network used in CNMA, each neuron in a layer is connected to each neuron in the previous layer. Such a network has one input layer, one output layer and zero or more hidden layers. When the values of neurons in the input layer are initialized, they are propagated forward to compute values of all neurons. The output layer can have multiple neurons allowing modeling of multi-output functions. Associated with the edge between two neurons is a weight. Associated with each neuron is a bias or intercept. The value of a hidden-layer neuron is a linear combination of its bias, values in the previous layer and weights of connecting edges, but passed through an activation function. Activation functions give neural networks the power to model nonlinear functions. We use the ReLU activation function $\max(0, x)$ because it can be converted into an MILP constraint using the big M method [27]. By also modeling the overall system requirement as another mixed integer linear constraint, scalable MILP solvers can be used to efficiently solve the neural network along with the requirement. To allow neural networks to model negative outputs, no activation function is applied at

the output layer.

We now illustrate the above plan with a short example. To model the equation $y = \max(x, 0)$ as an MILP, select a large number M and let an integer $d \in \{0, 1\}$. Then, $y = \max(x, 0)$ is equivalent to $(y \geq 0 \wedge y \geq x \wedge y \leq x + M * d \wedge y \leq M(1 - d))$. We now show how to model a whole neural network as an MILP.

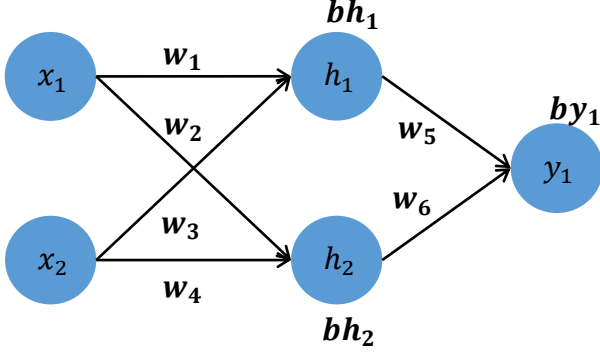


Figure 2. A fully-connected neural network.

The neural network in Figure 2 uses the ReLU activation function and can be modeled as:

$$\begin{aligned} h_1 &= \max(w_1 * x_1 + w_3 * x_2 + bh_1, 0) \wedge \\ h_2 &= \max(w_2 * x_1 + w_4 * x_2 + bh_2, 0) \wedge \\ y_1 &= w_5 * h_1 + w_6 * h_2 + by_1 \end{aligned}$$

Letting $M = 100000$ and d_1, d_2 integers $\in \{0, 1\}$, the equivalent MILP for this network, nn_milp , is:

$$\begin{aligned} nn_milp &= (h_1 \geq 0 \wedge \\ &h_1 \geq w_1 * x_1 + w_3 * x_2 + bh_1 \wedge \\ h_1 &\leq w_1 * x_1 + w_3 * x_2 + bh_1 + 100000 * d_1 \wedge \\ &h_1 \leq 100000 * (1 - d_1) \wedge \\ &h_2 \geq 0 \wedge \\ h_2 &\geq w_2 * x_1 + w_4 * x_2 + bh_2 \wedge \\ h_2 &\leq w_2 * x_1 + w_4 * x_2 + bh_2 + 100000 * d_2 \wedge \\ &h_2 \leq 100000 * (1 - d_2) \wedge \\ &y_1 = w_5 * h_1 + w_6 * h_2 + by_1) \end{aligned}$$

Let the above neural network model a blackbox function $F(x_1, x_2) = y_1$ and let $\phi(x_1, x_2, y_1), P(x_1, x_2, y_1)$ be an MILP objective function and constraint, respectively. Then, to optimize $\phi(x_1, x_2, y_1)$ subject to $F(x_1, x_2) = y_1 \wedge P(x_1, x_2, y_1)$, we can use an MILP solver to optimize $\phi(x_1, x_2, y_1)$ subject to $nn_milp \wedge P(x_1, x_2, y_1)$.

A central innovation of CNMA is that the neural network does not have to model F exactly to solve the optimization problem. To model it exactly would require an astronomical number of samples from F 's domain. Instead, CNMA tries to choose samples that are relevant to solving the optimization problem and are thus a tiny fraction of the number required for accurate modeling. After each sample, the neural network surrogate is reconstructed and the optimization problem solved again. The solution is used to compute the next promising sample and the step repeated till an acceptable solution is found.

IV. METHODOLOGY

CNMA solves the problem of finding x, y that optimize $\phi(x, y)$ such that $F(x) = y \wedge P(x, y)$ where F is a nonlinear function, x, y are vectors of discrete and continuous variables, ϕ is a linear function and P is a linear constraint. F is called the forward function. As shown in Figure 3, CNMA uses a Sample Generator to sample points in F 's domain, evaluates those points and creates a training set. These points are inputs to the neural network (NN) ReLU Regression Engine that outputs a neural network nn . This is transformed into an equivalent MILP $milp$ by the NN-MILP transformer. $milp$ is a surrogate or model of F based on current *samples*. An MILP solver solves $\phi(x, y)$ such that $milp \wedge P(x, y)$ is true. If a solution is not found, the Sampling Engine is called upon to extend *samples* with a new one in the hope of improving upon the current surrogate, and CNMA restarts. Otherwise, let (x^*, \hat{y}) be a solution. It is then checked for correctness, i.e., whether $P(x^*, F(x^*))$ holds. If it does, then the value of the objective function $\phi(x^*, F(x^*))$ is checked for acceptability, e.g., whether it is above or below a desired threshold or whether the evaluation budget has been reached. If the solution is acceptable, $(x^*, F(x^*))$ is output and CNMA halts. Otherwise, $(x^*, F(x^*))$ is added to *samples*. If $P(x^*, F(x^*))$ is false, then $(x^*, F(x^*))$ is also added to *samples*. Now, CNMA restarts. Note that CNMA can be used in pure constraint satisfaction mode by letting $\phi(x, y) = 0$ and in pure optimization mode by letting $P(x, y) = true$.

The addition of $(x^*, F(x^*))$ if $P(x^*, F(x^*))$ does not hold is a form of learning from the failure to produce a surrogate of F that intersects P . It has the effect of trying to restrict the sampling to only the part of F 's domain that is relevant to the satisfaction of P . Thus, the sampling of F is reduced by many orders of magnitude over the fine-grained sampling needed to learn F over its entire domain. Even if $P(x^*, F(x^*))$ does hold, adding it to *samples* in the hopes of improving upon $\phi(x)$ also restricts the sampling.

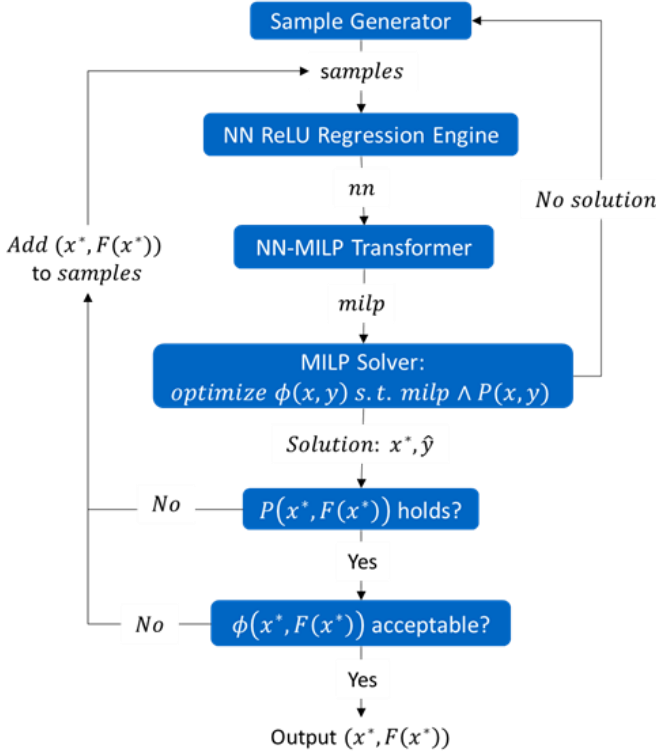


Figure 3. Sequential CNMA overview

For clarity, the above flowchart (and Algorithms 1, 2 and Figure 4) omit an important case: the failure to evaluate F for a given input either in the creation of the initial samples or in the evaluation of $P(x^*, F(x^*))$. In this case, CNMA just calls upon the Sample Generator to generate a new sample and restarts. Neural networks are resilient to missing data.

Algorithm 1 precisely defines the above plan.

Algorithm 1 CNMA, Single Forward Function

Input: a problem definition of the form $\max_{x,y} \phi(x,y)$ s.t. $y = F(x) \wedge P(x,y)$, a method to randomly sample candidate solutions $x \in X$, maximum number N of CNMA iterations. ϕ, P are linear, x, y are vectors of discrete and continuous variables, and F is a potentially nonlinear function available as a blackbox.

Output: a solution, (x^*, y^*) , to the above problem

function CNMA(ϕ, F, P, X, N)

$samples \leftarrow \{(x_i, F(x_i))\}_{i=1,2,\dots,n}$ where x_i denotes a random sample drawn from X
 $solutions \leftarrow$ empty list

for $i = 1, 2, \dots, N$:

$nn \leftarrow$ a fully connected ReLU regression network, i.e., with identity activation for the last layer, which takes in as input a vector $x \in X$ and attempts to predict $f(x)$; use $samples$ to train this neural network

$milp \leftarrow$ the mixed-integer linear program:

$$\max_{x,y} \phi(x,y) \text{ s.t. } nn_to_milp(nn) \wedge P(x,y)$$

$x^*, \hat{y} \leftarrow$ potentially infeasible solution to $milp$, obtained via an MILP solver

if (x^*, \hat{y}) is a feasible solution to $milp$:

$y^* \leftarrow F(x^*)$ // if F does not terminate within some time limit then F returns ∞
if y^* is finite:
 if $P(x^*, y^*)$ is satisfied:
 Append (x^*, y^*) to $samples$
 Append (x^*, y^*) to $solutions$
 else:
 Append (x^*, y^*) to $samples$
 endif
endif
else: // the solution to $milp$ is infeasible
 Append randomly drawn sample(s) $\{x_i, F(x_i)\}_{i=1,2,\dots}$ to $samples$
endif
return the best solution from $solutions$, sorting by $\phi(x,y)$
endfunction

It is possible that CNMA could get stuck in local optima. There are two methods of steering it away from them. The first is adding a constraint on an upper or lower bound of the objective function so that the MILP solver finds solutions satisfying that constraint. The second is to use multiple concurrent copies of CNMA, each producing a different surrogate and therefore adding different “good” points to $samples$. By pooling together these good points, the chances of finding the true optima can be improved. This method is a byproduct of Parallel CNMA that parallelizes sampling, training and solving to improve the quality and performance of the sequential version.

A. Parallel CNMA

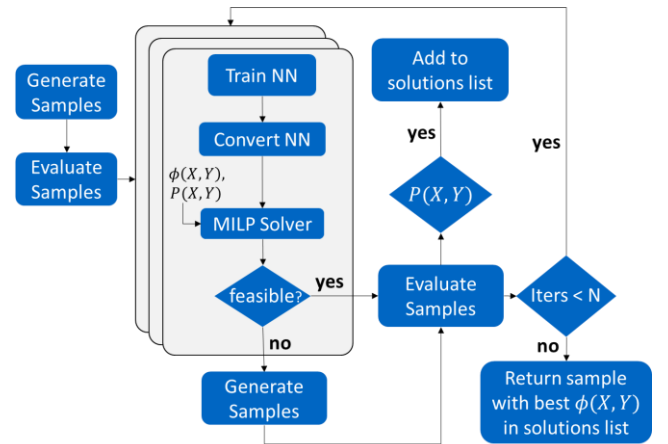


Figure 4. Parallel CNMA overview

As shown in Figure 4, the CNMA algorithm can also be parallelized by having multiple instances of CNMA run simultaneously while periodically sharing information with each other. During each iteration, each CNMA solver will use the existing evaluated samples as training data to create a surrogate model of the forward function, F . Each solver may use a different neural network architecture or initialize the neural network weights differently, causing each solver to end up with a unique MILP problem to solve and produce a different point to sample next. Because there are many different neural networks that all may fit the training data, running CNMA in

parallel allows us to explore more of these diverse surrogate models in a single iteration. At the end of each iteration, all evaluated samples are shared among the solvers. See Algorithm 2 for a precise definition of Parallel CNMA.

Algorithm 2 Parallel CNMA, Single Forward Function

Input: a problem definition of the form $\max_{x,y} \phi(x,y)$ s.t. $y = F(x) \wedge P(x,y)$, a method to

randomly sample candidate solutions $x \in X$, maximum number N of CNMA iterations, M parallel solvers. ϕ, P are linear, x, y are vectors of discrete and continuous variables, and F is a potentially nonlinear function available as a blackbox.

Output: a solution, (x^*, y^*) , to the above problem

function CNMA(ϕ, F, P, X)

$samples \leftarrow \{(x_i, F(x_i))\}_{i=1,2,\dots,n}$, where x_i denotes a random sample drawn from X

$solutions \leftarrow$ empty list

for $i = 1, 2, \dots, N$

$candidate_solutions \leftarrow$ empty list

parallel for $j = 1, 2, \dots, M$

$nn \leftarrow$ a fully-connected ReLU regression network (with any arbitrary architecture), which takes in as input a vector $x \in X$ and attempts to predict $F(x)$; use $samples$ to train this neural network.

$milp \leftarrow$ the mixed-integer linear program:

$\max_{x,y} \phi(x,y)$ s.t. $nn_to_milp(nn) \wedge P(x,y)$

$x^*, \hat{y} \leftarrow$ solution to $milp$, obtained, e.g., via an MILP solver

if (x^*, \hat{y}) is feasible:

$candidate_solutions[j] \leftarrow (x^*, \hat{y})$

$evals \leftarrow$ in parallel, compute $(x_i, F(x_i))$ for each $x_i \in candidate_solutions$

$n_{invalid} \leftarrow 0$

for $j = 1, 2, \dots, size_of(evals)$

$x^*, \hat{y} \leftarrow candidate_solutions[j]$

if (x^*, \hat{y}) is infeasible:

$n_{invalid} \leftarrow n_{invalid} + 1$

else:

Append (x^*, \hat{y}) to $samples$

if $P(x^*, \hat{y})$:

Append (x^*, \hat{y}) to $solutions$

In parallel, append $n_{invalid}$ randomly drawn sample(s) $(x_i, F(x_i))$ to $samples$

return the best solution from $solutions$, sorting by $\phi(x,y)$

endfunction

B. Illustrating CNMA

The Rastrigin function is a common benchmark problem for optimization methods because it is highly non-linear and has many local optima. We illustrate three different ways in which CNMA can be used to solve the optimization problem:

$$\max_{x \in [-5.12, 5.12]} F(x) = 10 + x^2 - 10 * \cos(2 * \pi * x)$$

The true maximum of $F(x)$ is 40.3533 at $x = -4.52299$ and $x = 4.52299$. Figure 5 shows the progression of CNMA at each iteration solving: maximize $\phi(x,y) = y$ s.t. $F(x) = y \wedge$

$-5.12 \leq x \leq 5.12$. CNMA first generates two initial samples in the domain of x to create the training set:

x	$F(x)$
-3.4950761251382723	32.210771821116786
-2.4368673278404436	25.161832324093915

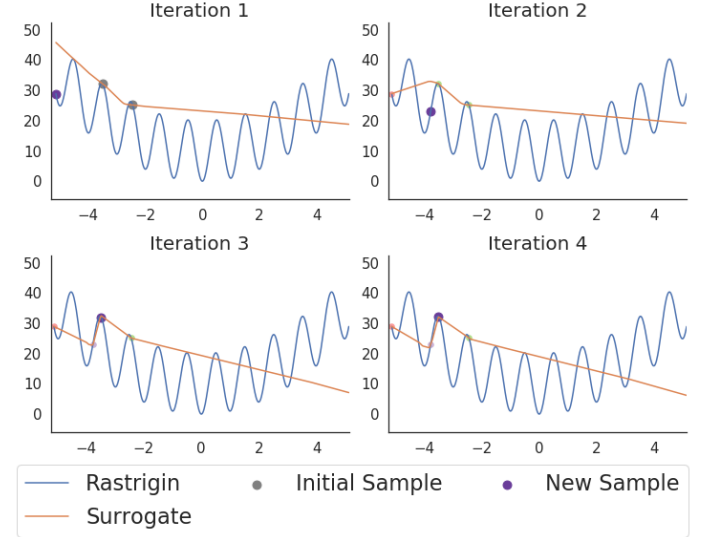


Figure 5. Maximizing Rastrigin

CNMA then learns a neural network from this set to create a surrogate of $F(x)$. Figure 5 shows the surrogate function plotted in orange. CNMA converts this neural network into an MILP and uses an MILP solver to solve it along with $P(x,y) = -5.12 \leq x \leq 5.12$ such that y is maximized.

During the first iteration, the solution found is $x = -5.12$. This is where the maximum of the orange curve is within x 's domain. After checking the solution against the correct definition of $F(x)$, the dot shown in purple is added to the training set and a new neural network is trained during Iteration 2. While CNMA is able to find a local maximum after just three iterations and five function calls, CNMA gets stuck here and a global maximum is not found even after 100 iterations.

To help CNMA explore outside this local maximum, we can use Parallel CNMA to add neural network diversity. Figure 6 shows how Parallel CNMA solves the same problem but is able to find the global maximum by using 10 different CNMA workers simultaneously. During the first iteration, 10 neural networks, each initialized with different weights, are trained on the same two initial samples. This creates 10 different MILP problems to be solved. Because each neural network is slightly different, each MILP problem produces a different solution. The eighth neural network predicts that the maximum value of the function is at $x = -4.5710$, which is close to one of the true maxima at $x = -4.52299$. Since all samples are shared among all parallel workers, by the next iteration each neural network predicts that the maximum is very close to the true maximum at $x = -4.52299$. After only three iterations, the best solution found is $x = -4.5219$, which has an objective function value of $y = 40.3531$.

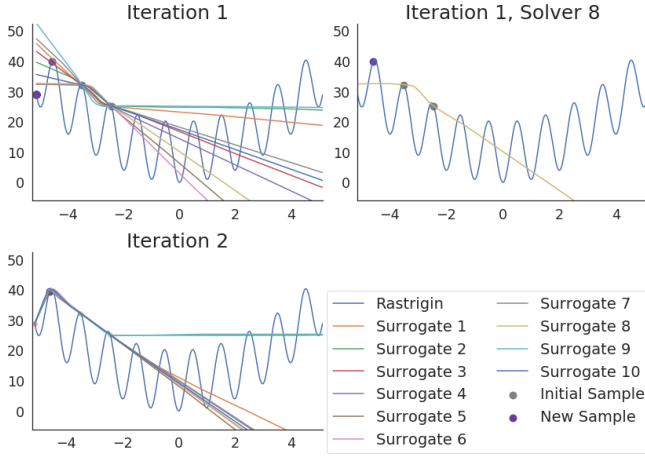


Figure 6. Maximizing Rastrigin with multiple CNMA solvers.

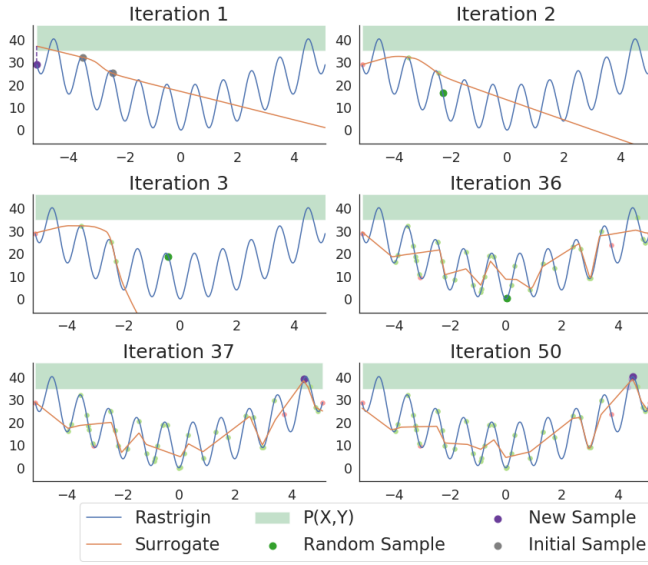


Figure 7. Maximizing Rastrigin with constraints

Another way to try to ensure CNMA does not get stuck in local maxima is to add a constraint to ensure that the objective function value is above a desired threshold. In Figure 7 is depicted the progression of CNMA with the added constraint $y \geq 35$. During Iteration 1, the MILP solver finds $x = -5.12$ because it maximizes the surrogate in orange and $P(x, y)$ (shaded in light green) is satisfied. However, when the solution is evaluated by the true function (shown in purple), $P(x, y)$ no longer holds. In the second iteration, there is no x such that the surrogate and $P(x, y)$ overlap. Thus, the MILP problem is infeasible and a random sample is evaluated instead (depicted as a green dot). Many random samples continue to be generated until Iteration 37, where the surrogate function again overlaps with $P(x, y)$. After evaluating the MILP solution through the true function, this time $P(x, y)$ is satisfied. This causes the surrogate function to continue to overlap with $P(x, y)$ during subsequent iterations. The solution $x = 4.5236$ with objective function $y = 40.3532$ is found after 50 iterations and 52 function calls (2 initial + one each for 50 iterations).

V. EXPERIMENTAL RESULTS

For seven nonlinear design problems of 8 (two problems), 10, 15, 36, 60 real-valued dimensions and one with 186 binary dimensions, we compare the performance of CNMA (with 1, 5, and 10 solvers) in parallel, and that of the `skopt` [31] implementation of BO/GP (abbreviated BO-S) and the `scipy.optimize` [33] implementation of NM (abbreviated NM-S), and also with Random Search. For neural networks, we use the `scikit-learn` package [39]. All these are stable, off-the-shelf packages. We use a commercial MILP solver. For BO-S, we use the expected improvement (EI) acquisition function, and the Matérn kernel. The following hyperparameters are automatically tuned by BO-S: (1) all kernel length scales, (2) covariance amplitudes, and (3) parameters of the i.i.d. Gaussian noise added to the kernel. For CNMA with 1 solver, we use a neural network architecture with two hidden layers of 35 and 10 neurons. For CNMA with 5 solvers, we use the same neural network architecture in addition to ones with single hidden layers of 10, 30, 35, and 50 neurons. We use the same architectures (each repeated twice) for CNMA with 10 solvers. For each benchmark, we allocate a fixed time budget for CNMA, BO-S, and NM-S and track the progress of the objective function with time and the number of function calls. In the objective function vs. function evaluation plots presented later, it is noticeable that each optimization algorithm performs a different number of function evaluations in a given amount of time. We also compare Random Search by randomly generating the maximum number of samples used by any one of the optimization methods which found valid solutions and tracking the progress of objective function with the number of function evaluations. Note, however, that BO-S did not return a solution for two problems and NM-S did not return one for three. For BO-S and NM-S, we model constraints as a penalty function. Some comparative visualizations are available at <https://collab.perspectalabs.com/nonlinearbenchmarks/>.

A. Designing a Wave-Energy-Propelled Boat

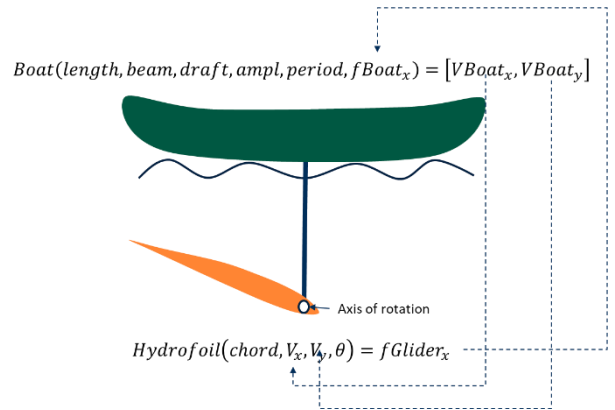


Figure 8. Structure of wave energy propelled boat. Note the recursive relationship between the input and output variables of Boat and Hydrofoil.

This example shows the ability of CNMA to optimize with functions that may fail to return a value for some inputs, as can happen with the `xfoil` [22] computational fluid dynamics simulator used here. Figure 8 indicates how the rise and fall of a boat floating on a wave pulls and pushes

at a hydrofoil below, causing a rotation about an axis. This rotation generates forward force during both the upward and downward wave motion; much like when swimmers flap flippers in a pool, their body is propelled forward. The marine robot is inspired by the Wave Glider [40]. The design problem is computing the dimensions of the boat and hydrofoil to maximize the steady-state forward sailing speed for a given wave condition. The equilibrium constraints are that the force generated by the hydrofoil equals that applied to the boat and that the glider and boat velocities are equal. An additional constraint is that the magnitude of the horizontal velocity be higher than that of the vertical velocity. Note the recursive relationship between the variables: force is an output of *Hydrofoil* but an input to *Boat* whereas velocities are outputs of the latter and inputs to the former.

The boat is modeled with two functions. The first is $f_{Hydrofoil}(ch, V_x, V_y, \theta) = f_{Glider}_x$ that computes the forward force output by a hydrofoil of length ch , moving through water at velocity V_x, V_y at an angle of attack θ . This is the force it applies to the boat. It is implemented with the computational fluid dynamics package `xfoil`. The second function is $f_{Boat}(length, beam, draft, ampl, period, f_{Boat}_x) = [V_{Boat}_x, V_{Boat}_y]$. It outputs the steady-state forward speed of a boat given its 3D dimensions: $length, beam, draft$, the amplitude $ampl$ and $period$ of the wave, and the forward force f_{Boat}_x applied to it by the hydrofoil. This function is computed by a program encoding a solution to a differential equation. The first two equilibrium constraints are enforced by eliminating V_x and V_y and consolidating the two functions into the CNMA forward function $F(x) = y$ where:

$$x = [length, beam, draft, ampl, period, f_{Boat}_x, ch, \theta]$$

$$y = [V_{Boat}_x, V_{Boat}_y, f_{Glider}_x]$$

F calls *Boat* to compute V_{Boat}_x and V_{Boat}_y and then inputs them to *Hydrofoil* to compute f_{Glider}_x . The third equilibrium constraint is now $f_{Boat}_x = f_{Glider}_x$. To tolerate small force differences, the equality is modeled as $|f_{Boat}_x - f_{Glider}_x| \leq \epsilon * f_{Boat}_x$ where ϵ is set to 5%. Note that a constraint with an absolute value can be modeled as a pair of linear constraints [41]. Finally, $P(x, y) = (|f_{Boat}_x - f_{Glider}_x| \leq \epsilon * f_{Boat}_x \wedge V_{Boat}_x \geq V_{Boat}_y)$ and $\phi(X, Y) = V_{Boat}_x$. In the optimization problem, $ampl$ and $period$ are set to 4 and 7, respectively.

With 30 initial samples and a budget of 2500 seconds, with 1, 5, and 10 solvers, CNMA is able to find a solution with a speed of 3.9036, 3.8993, and 3.8999 m/s, respectively. BO-S and NM-S are unable to find any feasible solutions given the same time budget. Out of 3890 randomly samples, none of them are valid solutions. Figure 9 and Figure 10 show the performance of CNMA with respect to time and number of function evaluations.

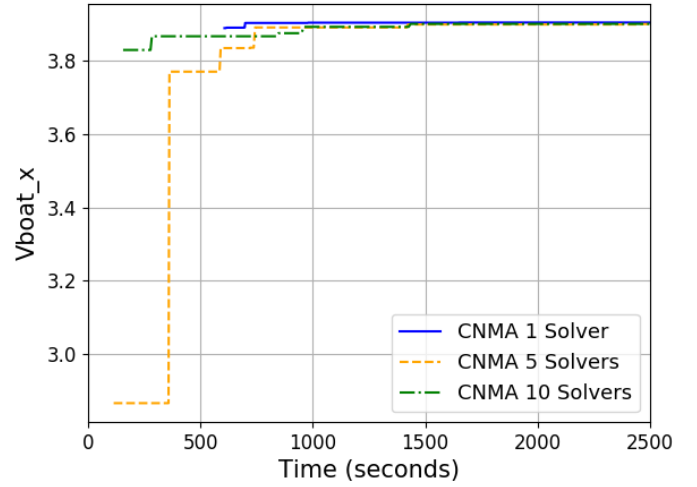


Figure 9. Boat velocity in the x direction vs. time for Wave-Energy-Propelled Boat. BO-S and NM-S are not shown since these are not able to find valid solutions.

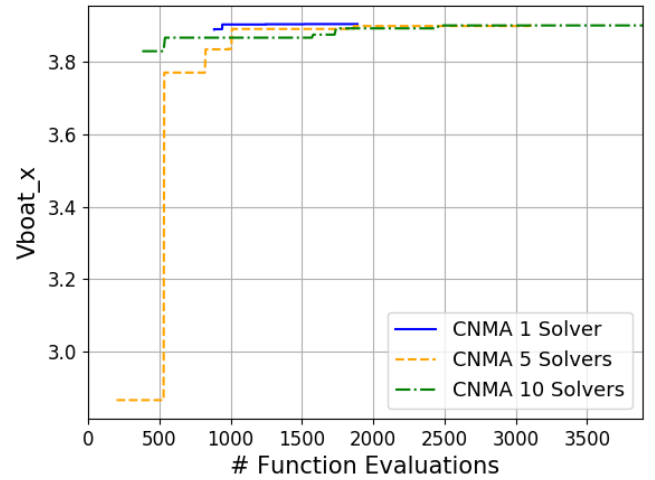


Figure 10. Boat velocity in the x direction vs. number of function evaluations for Wave-Energy-Propelled Boat. BO-S, NM-S, and Random Search are not shown since these are not able to find valid solutions.

B. OpenAI Gym's LunarLander: Robot System-Controller Codesign

Robots and their controllers are often designed separately. This can lead to design inconsistency whose resolution can be time-consuming. If robots can be efficiently reconfigured and their controllers efficiently designed, we raise the possibility of system-controller codesign

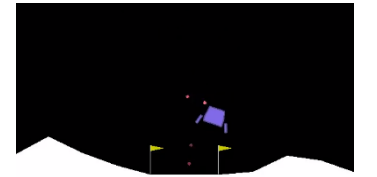


Figure 11. Lunar lander attempting to land on flat terrain between flagpoles

by solving a single optimization problem that encodes system and controller constraints and objectives. The lander we use, as depicted in Figure 11, is part of the robotic

benchmarks at OpenAI/Gym [42]. We assume that the controller is proportional-integral-derivative (PID)-based. Hence, the controller design problem reduces to finding optimal values for the PID coefficients. From a mothership, the module is ejected with a certain force and then its engines fire both vertically and horizontally to guide it towards landing on the flat pad between two flagpoles. Our goal is to compute the system and controller design and initial position and force that would maximize the reward while satisfying constraints on a successful landing, time to land and fuel usage.

The input vector to the CNMA forward function F is $X = [mep, sep, la, ld, lw, lh, lst, kp_alt, kd_alt, kp_ang, kd_ang, initial_x, initial_y, initial_fx, initial_fy]$. The variables $mep, sep, la, ld, lw, lh, lst$ are system design parameters denoting, respectively, main engine power, side engine power, leg away length, leg down length, leg width, leg height, and leg spring torque. The variables $kp_alt, kd_alt, kp_ang, kd_ang$ are controller design parameters denoting, respectively, the P and D values for the vertical and horizontal engine controllers. The I coefficient is set to 0. The variables $initial_x, initial_y, initial_fx, initial_fy$ are initial condition parameters, denoting, respectively, the initial position and force at the time of lunar lander ejection from the mother ship. The forward function $F(x) = y$ simulates the trajectory of the lander defined by its system design parameters, PID parameters and the initial conditions. It runs for a fixed number of time steps or until the lander lands or crashes. At each time step, it measures the “error,” i.e., the distance between its current position and the landing point, and using the PID values computes engine firing actions to guide the lander towards the landing point. It outputs $y = [fuel, time, success, reward]$ denoting, respectively, the fuel used, time taken to land, whether the landing is safe, and the reward, a measure of the quality of the landing, as defined by OpenAI/Gym. The codesign problem is now to maximize the objective function $\phi(x) = reward$ subject to $F(x) = Y \wedge P(x, y)$ where $P(x, y) = (success = 1 \wedge fuel \leq 75 \wedge time \leq 10)$.

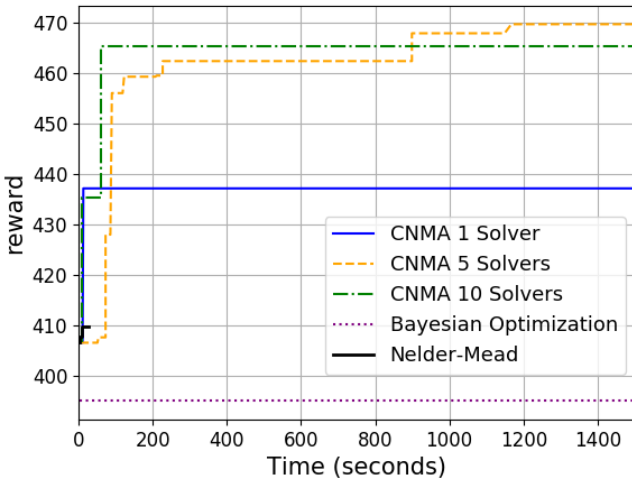


Figure 12. Reward vs. time for Lunar Lander. Note that NM-S stops after 28 seconds due to early convergence.

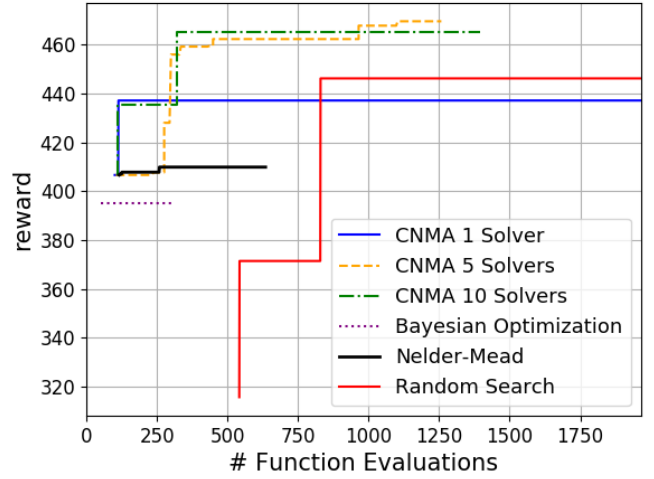


Figure 13. Reward vs. number of function evaluations for Lunar Lander.

With 100 initial samples and a time budget of 1500 seconds, CNMA finds solutions with rewards of 437.139, 469.589, and 465.136 with 1, 5, and 10 solvers, respectively. In the same amount of time, BO-S only finds a solution with a reward of 395.118 and NM-S only finds a solution with a reward of 409.857. Out of 1966 random samples, the best solution which meets the constraints has a reward of 446.199. Figure 12 and Figure 13 show the performance of CNMA, BO-S, NM-S and Random Search with respect to time and number of function evaluations.

C. Optimizing Hexapod Gaits

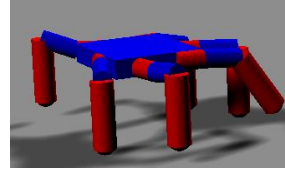


Figure 14. A hexapod

We now address a problem inspired by the work of [43] for adapting robot gait to failures in the field. The robot is six-legged with each leg consisting of three segments. Associated with each leg i is a vector of six parameters $(\alpha_i, \alpha_i, \phi_i, \phi_i, \tau_i, \tau_i)$ with each $\alpha, \phi, \tau \in [0, 1]$. These parameters determine, respectively, the amplitude phase and duty cycle of the walking signal sent to the first two legs every 30 ms. The walking signal for the third segment is the inverse of that for the second so does not need independent control parameters. The hexapod (as shown in Figure 14) controller is defined by the six parameters for each leg for a total of 36 parameters, and fully determines the hexapod gait. Using the hexapod simulator in [43], we define a CNMA forward function $hexapod(x) = y$ that takes a controller $x = [c_0, \dots, c_{35}]$ as input, simulates the hexapod gait for 5 seconds and outputs a vector $y = [speed_x, b_1, b_2, b_3, b_4, b_5, b_6]$ where $speed_x$ is the hexapod’s X-axis displacement in meters divided by 5.0 and each b_i is the fraction of the time leg i is in contact with the ground. Hexapod speeds above 0.20 m/sec are hard to find with Random Search [43].

If a hexapod leg is broken then we would like to find a new controller that can achieve a speed of above 0.20 m/sec while satisfying any new constraints on the movement. Let us assume leg 1 is broken. Then, we might constrain its

contact with the ground to be the least of that of all the legs. The problem is now: maximize *speed* subject to $\text{hexapod}([c_0, \dots, c_{35}]) = [\text{speed}, b_1, \dots, b_6] \wedge b_1 \leq b_2 \wedge b_1 \leq b_3 \wedge b_1 \leq b_4 \wedge b_1 \leq b_5 \wedge b_1 \leq b_6$ and stop when the speed is close enough to 0.20 m/sec. As can be seen above, the baseline controller does not satisfy the constraint.

We can try searching over $[0,1]^{36}$ for a new controller. However, another option is to search just in the neighborhood of the baseline controller. We change the bounds for each field in the baseline controller to be within 0.1 of its current value, subject to the lower bound being at least 0 and the upper bound at most 1.

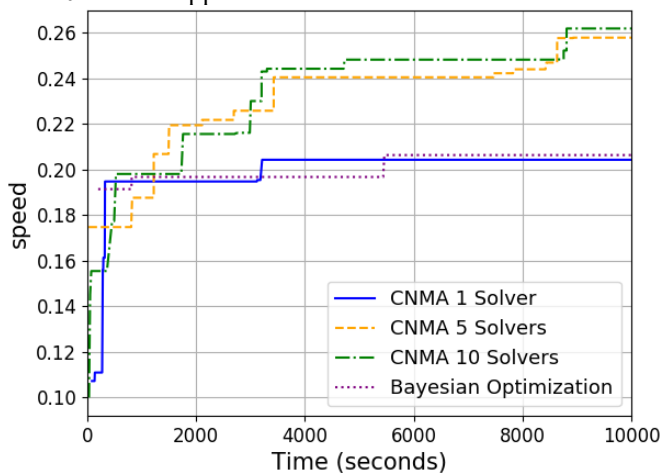


Figure 15. Speed vs. time for Hexapod. NM-S stops after 207 seconds due to early convergence. NM-S is not shown because it is not able to find any valid solutions.

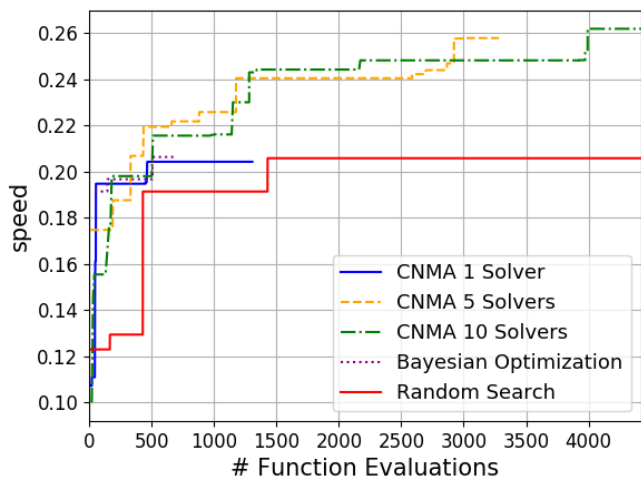


Figure 16. Speed vs. number of function evaluations for Hexapod. NM-S is not shown because it is not able to find valid solutions.

With two initial samples and a time budget of 10000 seconds, CNMA finds solutions with speeds of 0.2043, 0.2579, and 0.2619 m/sec with 1, 5, and 10 solvers, respectively. BO-S finds a solution with a speed of 0.2064 m/sec while NM-S is not able to find any valid solutions. Out of 4422 randomly generated samples, the best solution has a speed of 0.2058 m/sec. Figure 15 and Figure 16 show the performance of CNMA, BO-S, NM-S, and Random Search with respect to time and number of function evaluations.

D. Acrobot Design

The Acrobot [42], as shown in Figure 17, is a two-link robot arm with a single actuator placed at the elbow. Initially, the links hang downwards. The Acrobot's goal is to execute a series of actions that vertically orients and balances both links. The Acrobot problem is well-studied, and is known to be challenging to solve. In Figure 17, system design variables m_i , I_i , and l_{c_i} denote, respectively, the mass, moment of inertia, and center of mass

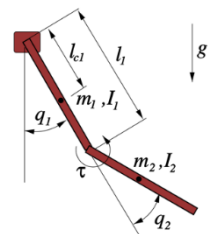


Figure 17. Acrobot schematic

location of link i . The CNMA function F takes as input a system design vector $x = [m_1, m_2, I_1, I_2, l_{c_1}, l_{c_2}, l_1, l_2]$, runs iterative linear-quadratic regulator (LQR) as our controller on an Acrobot system with this vector and returns $t_{\text{stabilize}}$, the total time taken to balance the system. The problem is to find a system design that minimizes $\phi(x, y) = t_{\text{stabilize}}$ subject to $F(x) = Y \wedge P(x, y)$ where:

$$P(x, y) = (I_1 = I_2 \wedge 0.1 \leq m_1, m_2 \leq 3.0 \wedge 0.1 \leq I_1, I_2 \leq 3.0 \wedge 0.1 \leq l_1, l_2 \leq 3.0 \wedge 0.3 \leq l_{c_1}, l_{c_2} \leq 0.7)$$

The constraint $I_1 = I_2$ reflects OpenAI/Gym's implementation of the Acrobot problem.

With 20 initial samples and a budget of 5000 seconds, CNMA finds solutions with objective function values 3.4, 3.2, and 2.8 with 1, 5, and 10 solvers, respectively. In the same amount of time, BO-S is able to find a solution with an objective function of 3.2 and NM-S is able to find a solution with an objective function of 8.6. Out of 500 randomly generated solutions, the best solution found has an objective function value of 4.2. Figure 18 and Figure 19 show the performance of CNMA, BO-S, NM-S, and Random Search with respect to time and number of function evaluations.

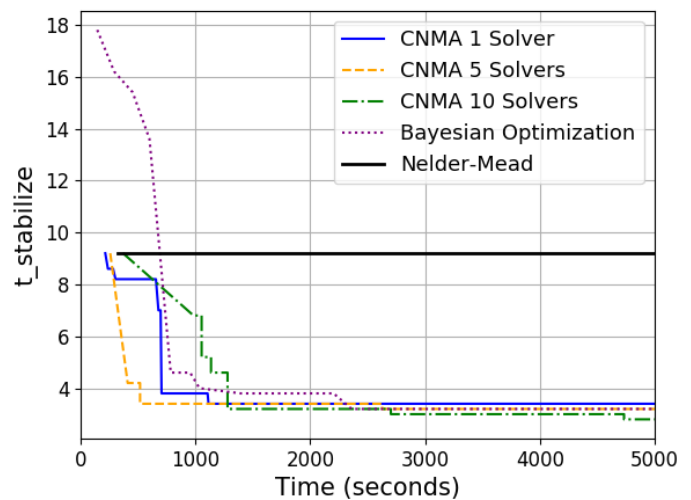


Figure 18. Stabilization time vs. time for Acrobot.

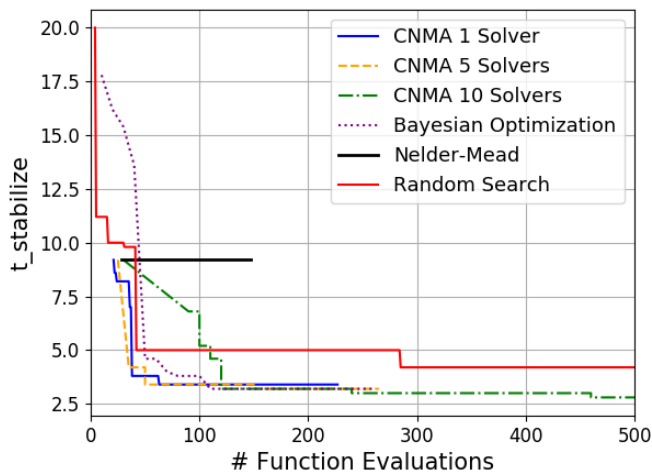


Figure 19. Stabilization time vs. number of function evaluations for Acrobot.

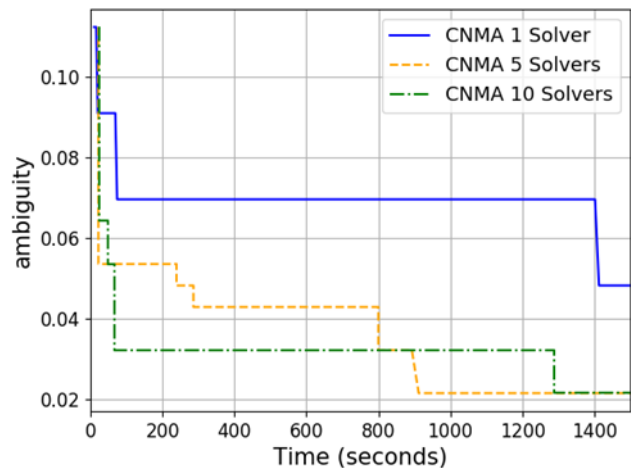


Figure 20. Ambiguity of the sensor placement vs. time for CNMA for sensor placement. BO-S, NM-S and Random Search are not shown since these are not able to find any solutions.

E. Optimal Sensor Placement for Power Grids

We now design a system in which all inputs are discrete but the output is continuous. Placing current and voltage sensors on a power grid can help identify which power lines are down during power outages. However, placing these sensors can be expensive and their number has to be limited. Given a limited sensor budget, the problem is to determine where to place the sensors such that their readings give the best chance of predicting the line failure pattern. We define a forward function F that takes in a sensor placement x of bits and outputs $y = [\textit{ambiguity}]$, the “ambiguity” of the placement. In x , if a sensor is placed at line i , then $x[i] = 1$ else $x[i] = 0$. For a given x , we simulate all single line failures and record the associated set of readings at the sensors placed in x . If a reading set appears more than once then it is ambiguous since more than one failure can cause it. We then divide the number of ambiguous reading sets by the total number of reading sets to compute $[\textit{ambiguity}]$ of x . Sensor readings are computed by the power line simulator OpenDSS [44], which takes in a model of the power grid, sensor placement, and a line failure pattern and outputs sensor readings. The objective function to minimize is $\phi(x, y) = \textit{ambiguity}$ subject to the constraint that the number of sensors placed at most meets some budget. For the Bus118 power grid with 186 power lines, and a budget of 50 sensors, the constraint is specified as $P(x, y) = \text{sum}(x) \leq 50$.

With 30 initial samples and a time budget of 1500 seconds, CNMA finds solutions with objective function values 0.04813, 0.02139, and 0.02139 with 1, 5, and 10 solvers, respectively. In the same amount of time, BO-S and NM-S are not able to find solutions that meet the constraints. Since these two only work with real-valued variables, we round their outputs to 1 or 0 to evaluate the forward function. Out of 460 randomly generated samples, none of them are valid solutions. Figure 20 and Figure 21 show the performance of CNMA, BO-S, NM-S and Random Search with respect to time and number of function evaluations.

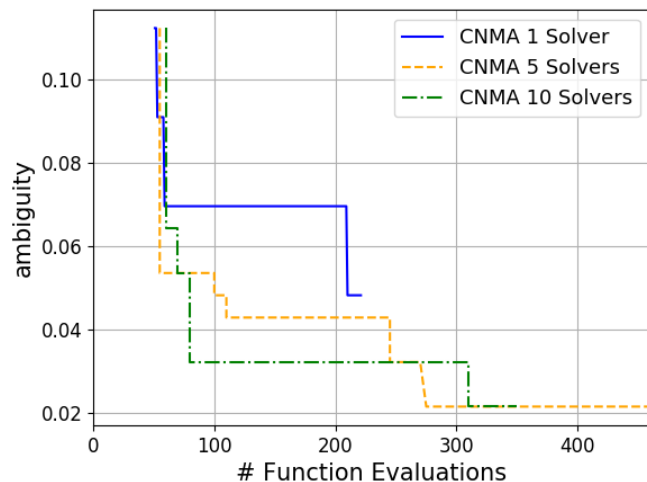


Figure 21. Ambiguity of the sensor placement vs. number of function evaluations for CNMA for sensor placement. BO-S, NM-S, and Random Search are not shown since these are not able to find any solutions.

F. Rover Path Planning

This problem, defined in [19], involves finding a trajectory, such as the one shown in Figure 22, for a robot with starting and end goal positions. The trajectory is specified by a set of 30 2D points that are fit by a BSpline to define a path. Each trajectory also has an associated cost which penalizes obstacle collisions and should be minimized. The CNMA function F takes as input the 2D coordinates of the 30 points (60 inputs) that define a path and outputs the cost of the trajectory. Each input ranges from 0.0 to 1.0. The objective is to maximize the negative cost of the trajectory.

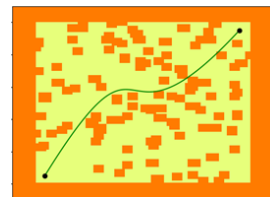


Figure 22. Path avoiding obstacles in x-y plane

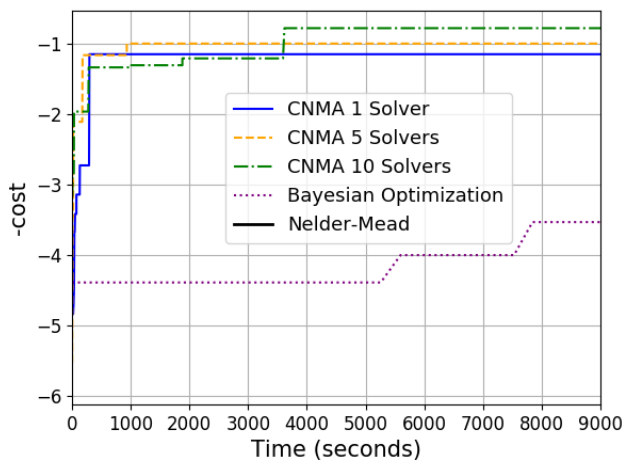


Figure 23. Negative cost vs. time for Rover Path Planning. Note that NM-S stops after 6 seconds due to early convergence.

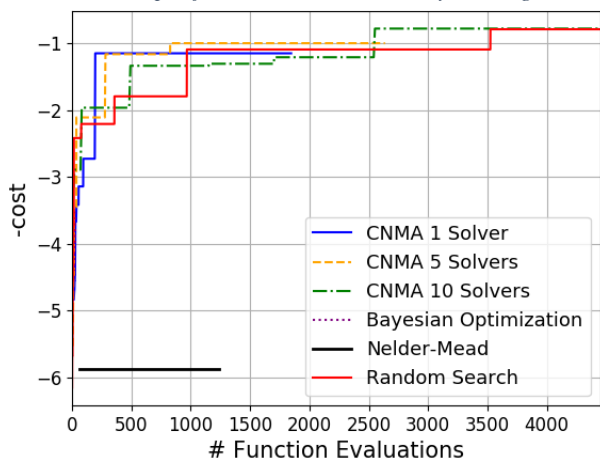


Figure 24. Negative cost vs. number of function evaluations for Rover Path Planning. Note that BO-S is only able to complete 30 function evaluations in the given time budget.

With two initial samples and a time budget of 9000 seconds, CNMA finds solutions with costs of 1.148, 0.997, and 0.778 with 1, 5, and 10 solvers, respectively. Given the same time budget, BO-S finds a solution with a cost of 3.530 and NM-S finds a solution with a cost of 5.867. Out of 4452 random samples, the best solution has a cost of 0.788. Figure 23 and Figure 24 shows the performance of CNMA, BO-S, NM-S, and Random Search with respect to time and number of function evaluations.

G. Polak3

This optimization benchmark [45] involves minimizing the maximum value of 10 different transcendental functions. The CNMA forward function $F(x) = y$ takes in 10 values, x_1, \dots, x_{10} , each $x_i \in [-1, 1]$, and outputs y as the maximum value of the 10 transcendental functions. The best reported minimum is 5.93. An example of such a function is

$$\begin{aligned}
 & 0.1428 * (e^{(x7-\sin(0.0+7.0+7.0))*(x7-\sin(0.0+7.0+7.0))}) \\
 & + 0.125 * (e^{(x8-\sin(0.0+8.0+8.0))*(x8-\sin(0.0+8.0+8.0))}) + \\
 & 0.1111 * (e^{(x9-\sin(0.0+9.0+9.0))*(x9-\sin(0.0+9.0+9.0))}) + \\
 & 0.1 * (e^{(x10-\sin(0.0+10.0+10.0))*(x10-\sin(0.0+10.0+10.0))}) + \\
 & 0.0909 * (e^{(x11-\sin(0.0+11.0+11.0))*(x11-\sin(0.0+11.0+11.0))}) \\
 & 0.5 * (e^{(x2-\sin(0.0+2.0+2.0))*(x2-\sin(0.0+2.0+2.0))}) + \\
 & 0.3333 * (e^{(x3-\sin(0.0+3.0+3.0))*(x3-\sin(0.0+3.0+3.0))}) + \\
 & 0.25 * (e^{(x4-\sin(0.0+4.0+4.0))*(x4-\sin(0.0+4.0+4.0))}) + \\
 & 0.2 * (e^{(x5-\sin(0.0+5.0+5.0))*(x5-\sin(0.0+5.0+5.0))}) + \\
 & 0.1666 * (e^{(x6-\sin(0.0+6.0+6.0))*(x6-\sin(0.0+6.0+6.0))}) +
 \end{aligned}$$

$$\begin{aligned}
 & 0.1428 * (e^{(x7-\sin(0.0+7.0+7.0))*(x7-\sin(0.0+7.0+7.0))}) \\
 & + 0.125 * (e^{(x8-\sin(0.0+8.0+8.0))*(x8-\sin(0.0+8.0+8.0))}) + \\
 & 0.1111 * (e^{(x9-\sin(0.0+9.0+9.0))*(x9-\sin(0.0+9.0+9.0))}) + \\
 & 0.1 * (e^{(x10-\sin(0.0+10.0+10.0))*(x10-\sin(0.0+10.0+10.0))}) + \\
 & 0.0909 * (e^{(x11-\sin(0.0+11.0+11.0))*(x11-\sin(0.0+11.0+11.0))})
 \end{aligned}$$

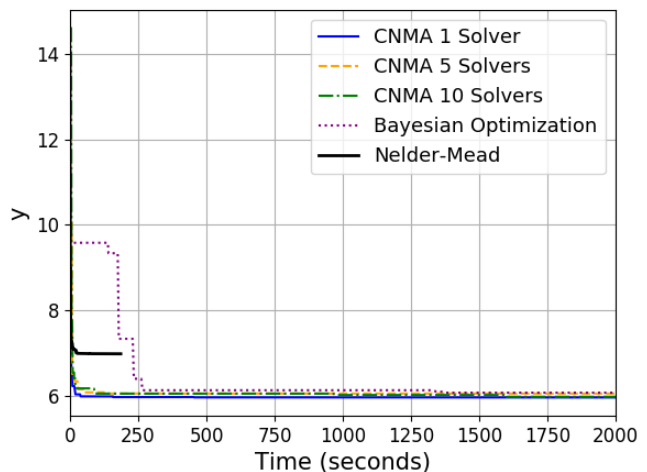


Figure 25. The maximum value of the 10 transcendental functions vs. time Polak3. Note that NM-S stops after 186 seconds due to early convergence.

With 20 initial samples and a time budget of 2000 seconds, with 1, 5, and 10 solvers CNMA finds solutions with objective function values 5.97, 6.06, and 5.98, respectively. Given the same time budget, BO-S finds a solution with an objective function value of 6.08 and NM-S finds a solution with an objective function value of 6.99. Out of 2680 randomly generated samples, the best solution has an objective function of 6.81. Figure 25 and Figure 26 show the performance of CNMA, BO-S, NM-S, and Random Search with respect to time and number of function evaluations.

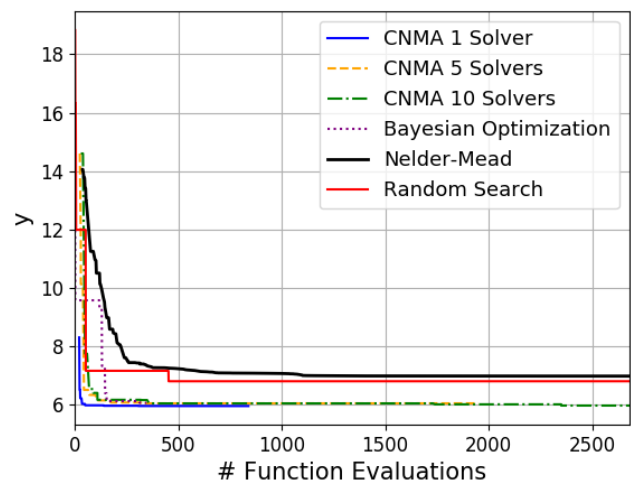


Figure 26: The maximum value of the 10 transcendental functions vs. number of function evaluations for Polak3.

H. Modeling Nonlinear Constraints and Objective Functions

To model a nonlinear constraint P , we add, for each nonlinear expression in P , an extra output to F denoting the value of the expression and then express P as a linear constraint on these

outputs. For example, we show how to solve a benchmark problem in [18]: minimize $g(x_1, x_2)$ subject to $c_1(x_1, x_2) \geq 0 \wedge c_2(x_1, x_2) \geq 0$ where $g(x_1, x_2) = x_1 + x_2$, $c_1(x_1, x_2) = 0.5 * \sin(2\pi(x_1^2 - 2x_2)) + x_1 + 2x_2 + 1.5$, $c_2(x_1, x_2) = -(x_1^2) - (x_2^2) + 1.5$. We define a function $F(x_1, x_2)$ that produces two outputs v_1, v_2 computing, respectively, $c_1(x_1, x_2)$ and $c_2(x_1, x_2)$. Then with CNMA we solve the problem of minimizing $x_1 + x_2$ subject to $F(x_1, x_2) = [v_1, v_2] \wedge v_1 \geq 0, v_2 \geq 0$. In 84 evaluations (10 initial + 74 additional), CNMA finds a solution of 0.6003. The minimum is 0.599. Our neural network architecture has 35 and 10 neurons in the two hidden layers. The important point to note is that we can solve this problem through specification, not by changing CNMA. If the objective function g had been nonlinear, we would have added an extra output to F and minimized that.

VI. CONCLUSIONS

System design tools are often only available as blackboxes with complex nonlinear relationships between inputs and outputs. This article presents CNMA, a new constrained optimization method for blackboxes for solving the inverse problem of finding designs from requirements on output.

CNMA's innovation is connecting the modeling power of neural networks and constraint-solving power of MILP solvers into a learning-from-failure feedback loop in such a way that they do much of the work for us, permitting straightforward implementations of several desirable features into a single, cohesive system: efficient surrogate function construction, sample efficiency, constraint solving without penalty functions, solving blackbox constraints, optimization with discrete and continuous variables, resilience to non-terminating function evaluations, and parallelism.

If a large and deep neural network is needed to model a complex function, its MILP equivalent may not be efficiently solvable. However, CNMA does not need to model the function in its entire domain. It only needs to model it in the part of the domain relevant to solving the constrained optimization problem. If this region is not too complex, a smaller neural network is adequate so that its MILP equivalent could be efficiently solvable. This region is automatically computed by CNMA. As we have seen, the largest network used had [35, 10] neurons in its hidden layers and most problems start with few tens of initial samples, some even with just two. In fact, a large or deep neural network may be detrimental to performance as it would overfit the small number of points CNMA samples.

CNMA is evaluated for seven nonlinear design problems of 8 (2 problems), 10, 15, 36 and 60 real-valued dimensions and one with 186 binary dimensions. It is shown that CNMA improves upon stable, off-the-shelf implementations of BO/GP (BO-S), Nelder Mead (NM-S), and Random Search by 1%-87% for a fixed time and function evaluation budget. Note, however, that BO-S did not return a solution for two problems and NM-S did not return one for three. Future research problems include introducing additional diversity, e.g., via bootstrapping, multi-function CNMA, finding a good initial neural network architecture and adapting it as new samples are created.

Acknowledgments. We greatly appreciate the assistance and feedback from Robert Vanderbei, John Chinneck, Nick Sahinidis, Matthias Poloczek, Jaime Fisac, Nicholas Kraus,

Taylor Njaka, Jeremy Cohen, Todd Huster, Mengdi Wang and Robert Gramacy during this research and paper writing.

REFERENCES

1. C. Rasmussen and C. Williams, Gaussian Processes for Machine Learning. The MIT Press, 2006. <https://bit.ly/2PRBDZ1>
2. J. Chinnek, Practical Optimization: A Gentle Introduction. <https://bit.ly/3eoIBid>
3. L. Rios and N. V. Sahinidis, "Derivative-free optimization: A review of algorithms and comparison of software implementations," J. Glob. Optim., vol. 56, p. 1247, 2013.
4. J. Roberts and M. Kochenderfer, Mathematical Optimization, 2014. <https://stanford.io/3qygM9V>.
5. J. Mueller, Optimizing Expensive Blackbox Simulations. <https://bit.ly/2OGQWmx>
6. S. Singer and S. Singer, "Efficient implementation of the Nelder–Mead search algorithm," Appl. Numer. Anal. Comput. Math., vol. 1, pp. 524-534, 2004.
7. R. Gramacy. Surrogates. CRC Press, 2020.
8. V. Ky, C. D'Ambrosio, Y. Hamadi, and L. Liberti, "Surrogate-based methods for black-box optimization," Int. Trans. in Operations Research, 2016.
9. M. Ahmed and S. Prince, Bayesian Optimization. Borealis AI. <https://www.borealisai.com/en/blog/tutorial-8-bayesian-optimization/>
10. R. Vanderbei. LOQO User's Manual – Version 4.05. <https://bit.ly/3qQR4xo>
11. NEOS Server: State-of-the-Art Solvers for Numerical Optimization. <https://neos-server.org/neos/>
12. NEOS Guide. <https://neos-guide.org/>
13. M. Powell, "A view of algorithms for optimization without derivative," Mathematics Today, vol. 43, 2007.
14. J. Gardner, G. Pleiss, K. Q. Weinberger, D. Bindel, and A. G. Wilson. "GPYtorch: Blackbox matrix-matrix Gaussian process inference with GPU acceleration," in Proc. Advances in Neural Information Processing Systems, 2018.
15. J. Hernandez-Lobato, M. Gelbart, R. Adams, M. Hoffman, and Z. Ghahramani, "A general framework for constrained Bayesian optimization using information-based search," J. Machine Learning Research, vol. 17, 2016.
16. D. Eriksson and M. Poloczek, "Scalable constrained Bayesian optimization," in Proc. Int. Conf. on Artificial Intelligence and Statistics, 2021.
17. S. Ariaifar, J. Coll-Font, D. Brooks, and J. Dy, "ADMMBO: Bayesian optimization with unknown constraints using ADMM," J. Machine Learning Research, vol. 20, 2019.
18. V. Picheny, R. Gramacy, S. Wild., and S. Le Digabel, "Bayesian optimization under mixed constraints with a slack-variable augmented Lagrangian," arXiv:1605.09466, 2016.
19. Z. Wang, C. Gehring, P. Kohli, and S. Jegelka, "Batched large-scale Bayesian optimization in high-dimensional spaces," in Proc. Int. Conf. on Artificial Intelligence and Statistics, 2018.
20. J. Want, S. Clark, E. Liu, and P. Frazier, "Parallel

- Bayesian global optimization of expensive functions,” arXiv:1602.05149, 2019.
21. K. Kandasamy, A. Krishnamurthy, J. Schneider, and B. Póczos, “Parallelised Bayesian optimisation via Thompson sampling,” in Proc. Int. Conf. on Artificial Intelligence and Statistics, 2018.
 22. Xfoil. Subsonic Airfoil Development System. <https://bit.ly/3rzsfh5>.
 23. D. Bertsekas, “On penalty and multiplier methods for constrained minimization,” SIAM J. Control and Optimization, vol. 14, no. 2, Feb. 1976.
 24. J. Nocedal and S. Wright. Penalty and Augmented Lagrangian Methods. In: Numerical Optimization. Springer Series in Operations Research and Financial Engineering. Springer, 2006.
 25. R. Fletcher and S. Leyffer, “Nonlinear programming without a penalty function,” Math. Program., Ser. A 91, 2002.
 26. L. Guilhoto. An Overview of Artificial Neural Networks for Mathematicians. <https://math.uchicago.edu/~may/REU2018/REUPapers/Guilhoto.pdf>
 27. M. Akintunde, A. Lomuscio, L. Maganti, and E. Pirovano, “Reachability analysis for neural agent-environment systems,” in Proc. Int. Conf. on Principles of Knowledge Representation and Reasoning, 2018.
 28. I. Pan, M. Babaei, A. Korre, and S. Durucan, “Artificial neural network based surrogate modelling for multi-objective optimisation of geological CO2 storage operations,” Energy Procedia, vol. 63, 2014.
 29. B. Grimstad and H. Andersson, “ReLU networks as surrogate models in mixed-integer linear programs,” arXiv:1907.03140, 2019.
 30. K. Deb, A. Pratap, S. Agarwal, and T. Meyarivan, “A fast and elitist multiobjective genetic algorithm: NSGA-II,” IEEE Trans. Evolutionary Computation, vol. 6, no. 2, pp. 182–197, 2002.
 31. P. Terway, K. Hamidouche, N. Jha. Fast design-space exploration of nonlinear systems Part II. arxiv:2104.02464, 2021
 32. scikit-optimize. <https://scikit-optimize.github.io/stable/>
 33. scipy.optimize. <https://docs.scipy.org/doc/scipy/reference/optimize.html>
 34. D. C. Liu and J. Nocedal, “On the limited memory BFGS method for large scale optimization,” Mathematical Programming, vol. 45, pp. 503–528, 1989.
 35. J. Snoek, O. Rippel, K. Swersky, R. Kiros, N. Satish, N. Sundaram, M. Patwary, Prabhat, and R. Adams, “Scalable Bayesian optimization using deep neural networks,” in Proc. Int. Conf. on Machine Learning, 2015.
 36. E. Daxberger, A. Makarova, M. Turchetta, A. Krause. “Mixed-variable Bayesian optimization”. arXiv:1907.01329, 2020.
 37. H. Lee, R. Gramacy, C. Linkletter, C. Gray. "Optimization subject to hidden constraints via statistical emulation." Pacific Journal of Optimization vol. 7.3, pp. 467-478, 2011.
 38. S. Hassantabar, Z. Wang, and N. K. Jha, “Synthesis of compact and accurate neural networks,” arXiv:1904.09090, 2019.
 39. scikit-learn. <https://scikit-learn.org/stable/>
 40. N. Kraus. Wave Glider Dynamic Modeling, Parameter Identification and Simulation. M.S. Thesis, University of Hawaii, Manoa, 2012.
 41. B. Granger, M. Yu, and K. Zhou. Optimization with absolute values, 2014, <https://bit.ly/3buDz1N>
 42. Open AI/Gym Classic Control Problems. https://gym.openai.com/envs/#classic_control
 43. A. Cully, J. Clune, D. Tarapore, et al. “Robots that can adapt like animals,” Nature, vol. 521, pp. 503–507, 2015.
 44. OpenDSS. Electrical power system simulation tool. <https://bit.ly/2O9aoZB>.
 45. Nonlinear minmax Problem in 11 variables, <https://bit.ly/38r2O39>



Sanjai Narain is Fellow and Chief Scientist at Perspecta Labs, Basking Ridge, NJ. He received his B.Tech. in EE from IIT Delhi in 1979 and his Ph.D. in CS from UCLA in 1988.



Emily Mak is Research Scientist at Perspecta Labs, Basking Ridge, NJ. She received her B.S. and M.S. in Applied Math from Johns Hopkins University in 2018.



Dana Chee is Senior Research Scientist at Perspecta Labs, Basking Ridge, NJ. She received her M.S. in Electrical Engineering from Howard University.



Brendan Englot is Geoffrey Inman Professor of Mechanical Engineering at Stevens Institute of Technology, Hoboken, NJ. He received his B.S., M.S. and Ph.D. in Mechanical Engineering from MIT in 2007, 2009, and 2012, respectively.



Kishore Pochiraju is Professor of Mechanical Engineering at Stevens Institute of Technology, Hoboken, NJ. He received his M. Tech. in Mechanical Engineering from IIT Kanpur and a Ph.D. from Drexel University in 1993.



Niraj K. Jha is Professor of Electrical Engineering at Princeton University, Princeton, NJ. He obtained his B.Tech. in E&ECE from IIT Kharagpur in 1981 and a Ph.D. in EE from University of Illinois at Urbana-Champaign, IL in 1985. He is a Fellow of IEEE and ACM.



Karthik Narayan is the CEO of Starfruit-LLC. He obtained his B.S. in Math/CS from Georgia Tech. in 2011 and a Ph.D. in CS/AI from University of California, Berkeley in 2016.